Available online at www.sciencedirect.com
ScienceDirect
Bioorganic & Medicinal Chemistry 15 (2007) 903–914
Bioorganic & Medicinal Chemistry

ABP688, a novel selective and high affinity ligand for the labeling of mGlu5 receptors: Identification, in vitro pharmacology, pharmacokinetic and biodistribution studies

Samuel Hintermann,[a] Ivo Vranesic,[a] Hans Allgeier,[a] Armin Brülisauer,[b] Daniel Hoyer,[a] Michel Lemaire,[b] Thomas Moenius,[b] Stephan Urwyler,[a] Steven Whitebread,[c] Fabrizio Gasparini[a,*] and Yves P. Auberson[a]

[a]*Novartis Institutes for BioMedical Research, 4002 Basel, Switzerland*
[b]*Novartis Pharma AG, 4002 Basel, Switzerland*
[c]*Novartis Institutes for BioMedical Research, 02139 Cambridge, USA*

Received 6 July 2006; accepted 19 October 2006
Available online 21 October 2006

Abstract—[^{11}C]ABP688 (**2**) has recently been demonstrated to be a useful PET tracer for in vivo imaging of the metabotropic glutamate receptors type 5 (mGluR5) in rodents. We describe here the identification and preclinical profiling of ABP688 and its tritiated version [^{3}H]ABP688, and show that its high affinity (K_d = 2 nM), selectivity, and pharmacokinetic properties fulfill all requirements for development as a PET tracer for clinical imaging of the mGlu5 receptor.

1. Introduction

Based on amino-acid sequence, pharmacology, and second messenger coupling, metabotropic glutamate receptors (mGluRs) have been clustered into three groups (I–III).[1] Group I receptors (mGluR1 and mGluR5) are coupled to the phospholipase C intracellular pathway, Group II (mGluR2 and mGluR3) and Group III (mGluR4, 6, 7, and 8) are negatively linked to adenylyl cyclase.

In contrast to the glutamate-gated ion channels (NMDA, AMPA, and kainate receptors), which mediate the glutamatergic neurotransmission in the CNS, mGlu receptors belong to the 'family 3' G protein-coupled receptors and have been shown to play a modulatory role in the glutamatergic synaptic transmission, either by regulating ion channel activity or by neurotransmitter release. The recent discovery of small molecules that selectively interact with receptors of Group I (mGlu1 and mGlu5) and II (mGlu2 and mGlu3) has facilitated significant advances in the understanding of the roles of these receptors in brain physiology and pathophysiology.[2]

The identification of MPEP (**1**, 2-methyl-6-(phenylethynyl)-pyridine, Fig. 1), a selective, non-competitive, and brain-penetrable mGlu5 receptor antagonist,[3] allowed the exploration of the therapeutic potential of mGlu5 receptor antagonism. Results from a variety of behavioral studies revealed that—with the exception of the benzodiazepines—mGlu5 receptor antagonists exhibit the widest and most robust anxiolytic activity in preclinical models seen to date.[4–6] Upcoming clinical studies, involving the use of specific mGlu5 receptor antagonists, should soon indicate whether the preclinical

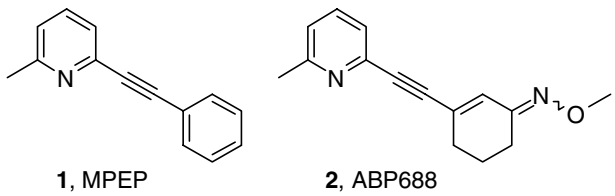

1, MPEP **2**, ABP688

Figure 1. Structures of MPEP and ABP688.

Keywords: Metabotropic glutamate receptor subtype 5; [^{3}H]ABP688; ABP688; PET imaging.
* Corresponding author. Tel.: +41 61 324 72 57; fax: +41 61 324 83 81; e-mail: fabrizio.gasparini@novartis.com

0968-0896/$ - see front matter © 2006 Elsevier Ltd. All rights reserved.
doi:10.1016/j.bmc.2006.10.038

anxiolytic-like effects translate into anxiolytic activity in man.

As comprehensive as it might be, the preclinical profile of a novel mGlu5 antagonist, as for other CNS drugs, does not allow an accurate prediction of the adequate drug dosing in humans. Positron emission tomography (PET) with receptor specific ligands is an imaging method which has been proven useful for studying these parameters in humans.[7,8]

To date, a number of mGlu5 receptor antagonists have been successfully used to label mGlu5 receptors in vitro.[9,10] However, the development of these ligands into useful PET tracers has so far not met with success[11,12] and only very recently a series of ^{11}C and ^{18}F-derivatives of MTEP and MTEB (2-methyl-4-phenylethynyl-thiazole), allowing PET imaging in rhesus monkey, has been described.[13]

In parallel to our discovery program aiming at the identification of mGlu5 receptor antagonists, we intended to identify a suitable PET ligand to support the clinical development of a pharmaceutical agent. Our target criteria for a potential PET ligand were: (1) a log *P* below 4; (2) an easy radiolabeling in the last synthesis step; (3) a high affinity (<10 nM) for mGluR5 and selectivity (>100-fold) over other receptors; (4) a rapid brain uptake and elimination; and (5) the absence of brain-penetrating radiolabeled metabolites. In order to allow for displacement studies and for determination of receptor occupancy by therapeutic drug candidates, any potential tracer would have to be competitively and fully displaced by drug candidates binding to the allosteric binding pocket at the mGlu5 receptor.

Initially, a series of PET candidates was synthesized based on the prototypic antagonist MPEP. A ^{11}C or ^{18}F label was introduced in positions C-3 of the phenyl ring or C-6 of the pyridine ring, which were shown to tolerate modifications without compromising the affinity for the allosteric binding site.[14,15] Four of these initial derivatives were tested in vivo in rat to determine their brain uptake and distribution but failed to meet the target profile, by exhibiting a combination of a relatively high lipophilicity, high non-specific binding, insufficient affinity or limited metabolic stability.

We subsequently revisited the library of compounds which had been synthesized during the medicinal chemistry program for mGluR5 antagonists and we focused on a series of derivatives with a cyclohexenone oxime instead of the aromatic ring contained in MPEP. The introduction of an oxime significantly decreased lipophilicity and improved water solubility, as compared to the precursor series. The most promising candidate identified was ABP688 (**2**), a high affinity and selective mGluR5 antagonist with a calculated log *P* of 2.4 (Fig. 1).

Since this compound fulfilled all of our criteria in terms of physicochemical properties, we decided to further explore its potential as a PET imaging ligand for the mGlu5 receptor. Here, we report on the preclinical characterization of ABP688 and its tritiated species [^{3}H]ABP688. This characterization allowed the selection of this ligand for development as a PET tracer.[16]

2. Chemistry

2.1. Synthesis of ABP688 (*2*) and its labeling precursor 7

The synthesis of ABP688 (**2**) and of the precursor of [^{3}H]ABP688, oxime **7**, started from commercially available 2-bromo-6-methyl-pyridine. A Sonogashira[17] cross coupling with 2-methyl-3-butin-2-ol yielded the tertiary alcohol (**3**), which was easily and in good yields converted into the alkynyl-pyridine (**4**), by base-catalyzed acetone elimination (Scheme 1). A second Sonogashira[18] coupling with 3-bromo-cyclohex-2-enone (**5**)[19] led directly to ketone **6**, which was then readily transformed into the labeling precursor **7** (*E*/*Z*-mixture 1.6:1) by base-catalyzed oxime formation with hydroxylamine hydrochloride. Similarly, oxime formation with *O*-methyl-hydroxylamine led to ABP688 (**2**) in excellent yield, as a mixture of *E*/*Z*-isomers (ca. 1.5:1). The stereochemical assignment of the ABP688 isomers was based upon a ROESY[20,21] peak between the olefinic H(2)-proton and the methyl-group in the *Z*-isomer, and upon the expected high field shift (123.1 ppm) in the ^{13}C-resonance of C(2) for the *Z*-isomer when compared to the *E*-isomer (130.8 ppm). The assignment of the two isomers of **7** was made by analogy with ABP688.

In summary, we could efficiently synthesize both ABP688 (**2**) and the labeling precursor [^{3}H]ABP688, oxime **7**, in four steps and excellent overall yields of 53%, starting from commercially available 2-bromo-6-methyl-pyridine.

2.2. Physicochemical properties and stability of ABP688

ABP688 is a low molecular weight molecule (mw = 240.3) with measured log *P* and log *D* (pH 6.8) of 3.4, both one unit above the calculated value, but still within an acceptable range (<4). Its pK_a is 3.8, and its solubility in water (120 mg/L at pH 6.8) is largely sufficient for an iv formulation. There was no decomposition of ABP688 or of **7** observable by HPLC after one week at 80 °C as a powder or in buffer suspension at pH 7.4. Precursor **7** is stable under conditions used for radiolabeling with ^3H (Scheme 2) and ^{11}C (DMF, 5 min at 90 °C).[16]

2.3. Radiosynthesis of [^{3}H]ABP688

Tritiated ABP688 was synthesized by reacting the preformed potassium salt of oxime **7** with [^{3}H]-methyl iodide at 120 °C for 2.5 h (Scheme 2). The product was isolated after purification by semi-preparative HPLC (Nucleosil 100-3 C-18 HD) as an *E*/*Z*-mixture (ca. 4:1) and stored as a solution in acetonitrile at −20 °C.

By careful optimization of the labeling procedure,[16] consistent isomeric ratios of >10:1 in favor of the more potent *E*-isomer could be obtained (data not shown).

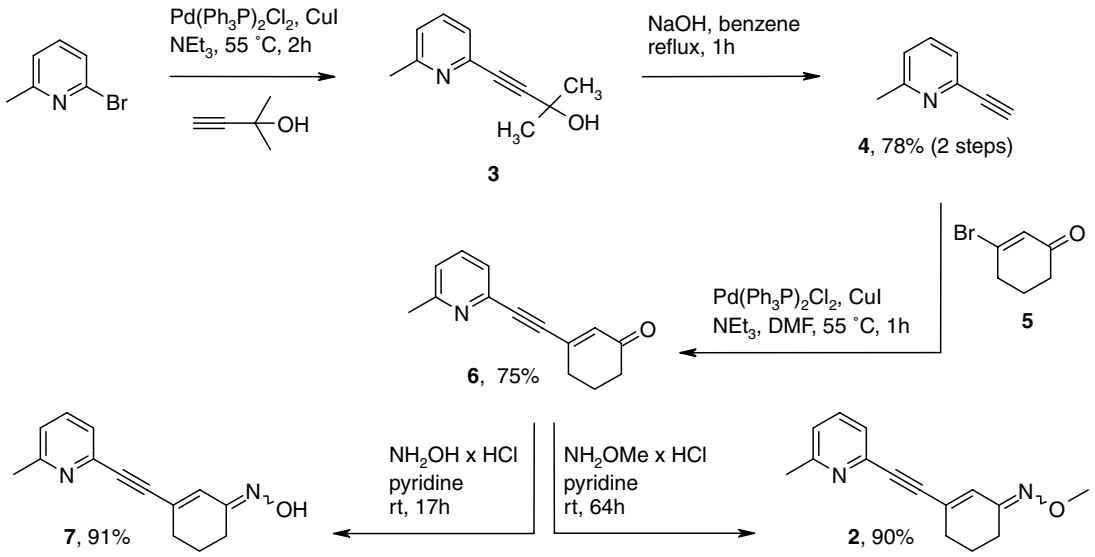

Scheme 1. Synthesis of ABP688 (**2**, 3-(6-methyl-pyridin-2-ylethynyl)-cyclohex-2-enone *O*-methyl-oxime) and the labeling precursor 3-(6-methyl-pyridin-2-ylethynyl)-cyclohex-2-enone oxime (**7**).

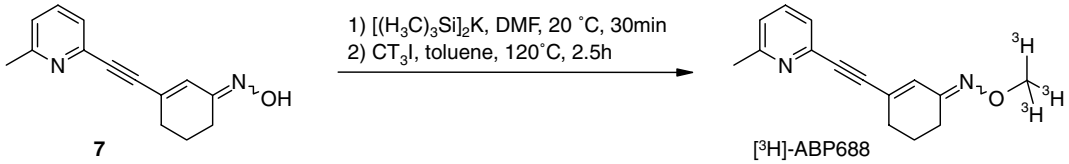

Scheme 2. Radiosynthesis of [^{3}H]ABP688: radiochemical purity: 99.4%, specific activity: 2.83 TBq/mmol (11.78 MBq/μg).

3. Pharmacological properties and evaluation as potential PET tracer

3.1. Potency and selectivity in functional assays

ABP688 was originally shown to be a potent antagonist of quisqualate-induced phosphoinositol (PI) accumulation in L(tk-) cells expressing recombinant human mGluR5 (hmGluR5), with an IC_{50} value of 2.4 nM (95% CI: 0.5–12 nM) (Fig. 2A). In the same preparation, ABP688 completely inhibited glutamate-induced calcium release with an IC_{50} value of 2.3 nM (95% CI: 2.1–2.5) nM (data not shown) and had no effect, up to 10 μM, on ATP-induced PI accumulation via stimulation of endogenously expressed purinergic receptors in hmGluR5-expressing cells (Fig. 2A), or on quisqualate-induced PI accumulation in hmGluR1-expressing cells. ABP688 had no effect on basal PI levels in hmGluR5- or hmGluR1-expressing cells (Fig. 2B).

3.2. [^{3}H]-M-MPEP displacement in membranes of hmGluR5-expressing cells

The affinity of ABP688 for the allosteric binding site in the transmembrane domain of mGluR5[22] was determined in a radioligand competition assay using [^{3}H]-M-MPEP.[9] In membranes prepared from L(tk-) cells expressing recombinant human mGluR5 (hmGluR5),[23] ABP688 fully displaced the binding of [^{3}H]-M-MPEP in a concentration-dependent manner (Fig. 3) with an IC_{50} value of 7.0 nM (95% CI: 6.1–8.1), or a corresponding K_i of 3.5 (3.1, 4.0) nM. The Hill coefficient was -0.92 ± 0.10 (±95% CI).

3.3. Receptor binding panel

The in vitro binding affinities of ABP688 for a variety of CNS GPCR receptors, ion channels or transporters were determined according to standard filtration methods.[24] ABP688, at concentrations of 1 and 10 μM, did not bind to any of the tested receptors or transporters, confirming the high degree of selectivity of ABP688 (details are available as Supplementary information).

3.4. Binding characteristics of [^{3}H]ABP688 in vitro

The characteristics of the binding of [^{3}H]ABP688 to native mGlu5 receptor were determined in membranes prepared from rat whole brain tissue. The observed association and dissociation time courses were well described by mono-exponential models, the respective rate constants were $k_{obs} = 0.103 \pm 0.006$ ($n = 3$) and $k_{-1} = 0.075 \pm 0.006$ min^{-1}($n = 5$). The calculated association rate constant k_1 was 0.07 nM^{-1} min^{-1}. From these values, an equilibrium binding constant K_d of 1.07 nM was calculated. The specific binding of [^{3}H]ABP688 was saturable and adequately described by a single-binding site model, with B_{max} and K_d values of 0.87 ± 0.096 pmol/mg protein and 2.3 ± 0.34 ($n = 4$) nM, respectively. (Fig. 4A–C).

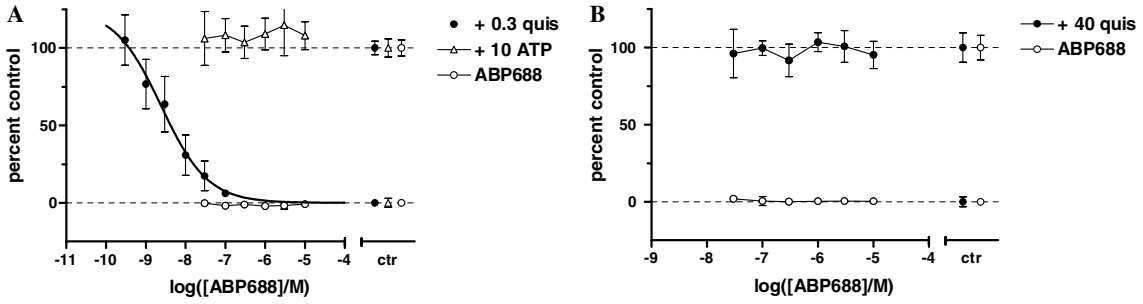

Figure 2. Effects of ABP688 on PI accumulation in cells expressing recombinant hmGluR5 (A) and hmGluR1 (B). (A) ABP688 fully inhibits quisqualate-stimulated (filled circles, 0.3 μM), but not ATP-stimulated (empty triangles, 10 μM) PI accumulation. Applied alone, ABP688 has no effect on basal PI accumulation (empty circles). Symbols offset to the left indicate respective normalized positive and negative controls ± SD. (B) Absence of effects on quisqualate-stimulated (filled circles, 40 μM) PI accumulation and basal PI levels (empty circles) in hmGluR1-expressing cells. All data sets shown represent percent control ± SD of $n = 3$ independent determinations, each performed in triplicate.

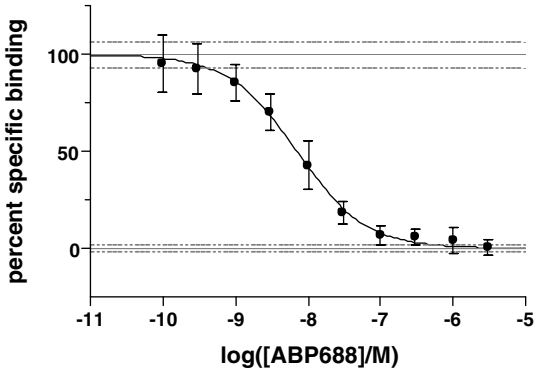

Figure 3. Concentration dependence of [^{3}H]-M-MPEP displacement by ABP688 in membranes prepared from hmGluR5-expressing cells. Data show percentage ± SD of specific binding of [^{3}H]-M-MPEP (2 nM). Non-specific binding was determined in the presence of 1 μM unlabeled M-MPEP. Data were obtained from $n = 2$ independent determinations, each performed in triplicate. Solid (± dashed) horizontal lines indicate normalized total and non-specific controls (±SD). Solid curve was obtained by fitting the logistic equation to the pooled data set, best-fit parameters and respective 95% confidence intervals are given in text.

In a further series of experiments, we utilized [^{3}H]ABP688 to determine the affinities of ABP688, MPEP, M-MPEP as well as CPCCOEt, an mGluR1 antagonist, to membrane preparations of hmGluR5-expressing cells and rat whole brain tissue. In both preparations, ABP688, MPEP, and M-MPEP fully displaced [^{3}H]ABP688 in a concentration-dependent manner with Hill coefficients near negative unity, while CPCCOEt had no appreciable effect on [^{3}H]ABP688 binding up to 10 μM (Fig. 5 and Table 1, for respective affinities). The solvent, DMSO, had no effect on binding (not shown). The near-equality of the respective binding affinities of APB688, MPEP, and MPEP to hmGluR5 and rat brain membranes indicated that there are no apparent species differences between recombinant human and native rat receptors in vitro.

3.5. Autoradiography in rat brain slices

In vitro autoradiography is an established method to determine the binding characteristics of a radioligand and the distribution of the labeled sites. In rat brain slices, incubation with 5 nM (70 Ci/mmol) of [^{3}H]ABP688 gave rise to a regionally differentiated binding pattern (Fig. 6A, left panels). The binding was displaceable by MPEP (10 μM), and the remaining (non-specific) binding was found to be nearly indistinguishable from background (Fig. 6).

High-to-medium specific binding was observed (in descending rank order) in nucleus accumbens, caudate putamen, hippocampus, olfactory tubercle, amygdala, and occipital and frontal cortices; low-to-near background binding was found in thalamus, hypothalamus, midbrain, pons-medulla, and cerebellum (Fig. 7). This pattern is consistent with autoradiographic results obtained with [^{3}H]methoxy-PyEP,[10] as well as mGluR5 expression patterns obtained with immunocytochemistry using mGluR5-specific antibodies[25,26] or mGluR5 mRNA distribution as determined with in situ hybridization.[27] Taken together, our present findings of a good (qualitative) correlation between [^{3}H]ABP688 binding and mGluR5 expression, in combination with low unspecific binding in native brain tissue, encouraged further profiling in vivo.

3.6. Blood distribution, plasma protein binding, and in vitro metabolism

The assessments were performed using [^{3}H]ABP688 with the objective of allowing a pharmacokinetic scaling from animal to man.

3.6.1. In vitro blood distribution. [^{3}H]ABP688 was stable when incubated in plasma at 37 °C and equilibrated rapidly between plasma and blood cells at 37 °C. The blood distribution was independent of concentration but slightly species-dependent, as illustrated by the fraction present in plasma of 76% in rat and 92% in human. The blood to plasma concentration ratios were 0.74 and 0.57 in rat and human, respectively. The characteristics of the blood distribution of [^{3}H]ABP688, that is, large fraction of the compound present in plasma compartment, independent of concentration, support the use of plasma concentrations to estimate the input function for PET studies.

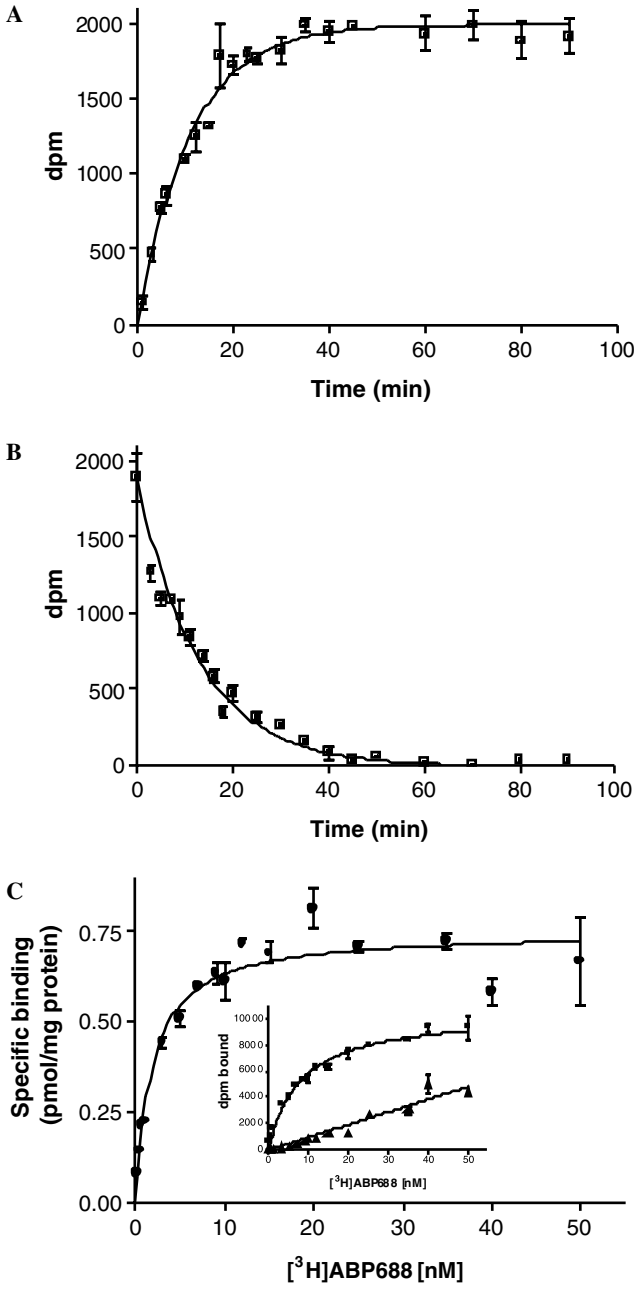

Figure 4. In vitro binding characteristics of [^{3}H]ABP688 in rat brain membranes. (A) and (B), association and dissociation kinetics of 0.4 nM [^{3}H]ABP688 binding. A mono-exponential model was used to derive apparent association and dissociation rate constants. The corresponding best-fit curves are depicted by solid curves. The data shown are from typical experiments, each performed in triplicate. (C) Saturation binding (inset, total and non-specific binding). The means of the kinetic or equilibrium binding parameters derived from several experiments are given in the text.

3.6.2. Plasma protein binding. The fraction of [^{3}H]ABP688 bound to plasma proteins was independent of concentration from 50 to 500,000 pg/mL, the average unbound fraction in plasma was higher in rat (6.8%) than in man (4.4%) in accordance with the stronger partitioning into blood cells.

3.6.3. Metabolic stability. [^{3}H]ABP688 was incubated with liver microsomes from rat and man. The metabolic stability was assessed by calculation of the intrinsic clearance CLint: the intrinsic clearance was medium to high in rat and human (roughly 150 μL/min/mg). HPLC analysis with radioactivity detection indicated oxidative hydroxylation to be the main metabolic pathway, leading to formation of tritiated water and four mono-hydroxylated metabolites. The exact positions of the hydroxy group could not be determined from the available LC–MS/MS data. No human-specific metabolites were detected when compared to rat.

3.7. Disposition of [^{3}H]ABP688 in rat following an intravenous microdose injection

The main objective of this pharmacokinetic study was to establish the disposition of ABP688 in plasma and brain of rats.

3.7.1. Pharmacokinetics. After a 4 μg/kg [^{3}H]ABP688 intravenous application, plasma concentrations declined rapidly (Fig. 8, left panel). Compartmental analysis according to a bi-exponential model resulted in plasma half-lives of approximately 5 min ($t_{1/2}$,1) and 1 h ($t_{1/2}$,2), respectively, where the fraction of AUC associated with the second half-life amounted to 59%. Since [^{3}H]ABP688 was stable when incubated in blood or plasma at 37 °C and only trace amounts of parent compound were detected in excreta, its elimination occurred almost exclusively by metabolism. Indeed, already 5 min. after administration, the fraction unchanged in plasma had decreased to 34% of plasma radioactivity, whereas the AUC of parent drug represented merely 1.4% of the AUC for total radioactivity. The blood clearance value of ABP688 (60 mL/min) was close to the cardiac output in rat indicating an important contribution of extra-hepatic metabolism, possibly located in the lung. The penetration of [^{3}H]ABP688 into the brain was rapid and extensive, and resulted in brain to plasma ratios of up to 20. Total radioactivity and parent compound concentrations in the brain were similar (Fig. 8, right panel), indicating that the proportion of radiolabeled metabolites entering the brain was negligible. The parallel decline of brain and plasma levels, with terminal half lives of 1.1 and 1.0 h, respectively, suggested passive diffusion at the blood–brain barrier.

3.7.2. Tissue distribution. The fraction of [^{3}H]ABP688 escaping a rapid elimination was largely distributed into tissues as indicated by the volume of distribution (VSS = 11 L/kg). At 5 min post-dose the highest tissue concentration of [^{3}H]ABP688 (21 pmol/g) was observed in the brain. At this time, the amount of parent drug left in the body represented only 21% of the administered dose, with a considerable fraction (0.8% of dose) present in the brain (Fig. 9). The next highest [^{3}H]ABP688 concentration occurred in fat tissue where the concentration measured between 5 min and 2 h post-dose corresponded to 6–10% of the administered dose.

No brain penetration of metabolites and no active transports of ABP688 from and to the brain were observed. These rat results predict a favorable human PK profile for ABP688 as PET ligand.

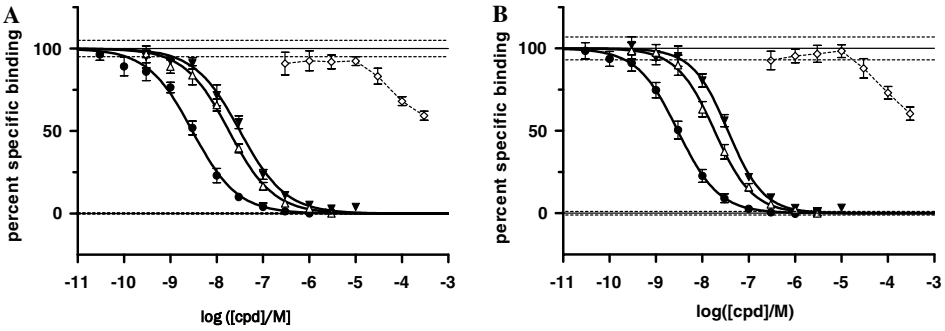

Figure 5. Concentration dependence of [^{3}H]ABP688 displacement by ABP688 (filled circles), M-MPEP (empty triangles), MPEP (filled triangles), and CPCCOEt (empty diamonds) in membranes prepared from whole rat brain (A) or cells expressing recombinant human hmGluR5 (B). Data show percentage ± SD of specific binding of 1.5 nM [^{3}H]ABP688. Non-specific binding was defined in the presence of 10 μM M-MPEP. Solid (±dashed) horizontal lines indicate normalized total and non-specific controls (±SD). Best-fit curves were obtained by fitting the logistic equation to the pooled data sets, see Table 1 for respective best-fit parameters and their 95% confidence intervals.

Table 1. Binding affinities (in nM) of MPEP, M-MPEP, and CPCCOEt in membrane preparations of hmGluR5-expressing cells and rat whole brain

	Membranes from L (tk-) cells expressing hmGluR5	*N*	Membranes from whole rat brain	*N*
Compound	K_i (95% CI) (nM)	*n*	K_i (95% CI) (nM)	*n*
M-MPEP	10 (9.2, 11)	3	11(9.8, 13)	3
MPEP	20 (17, 23)	3	19(16, 23)	3
ABP688	1.7 (1.5, 1.8)	7	1.8(1.5, 2.2)	7
CPCCOEt	>100,000	3	>10,000	3

4. Discussion

Initial efforts to identify a mGluR5-selective PET tracer based on the structural framework of the selective antagonist MPEP failed to produce a valid PET tracer. It is only very recently that a first series of ^{11}C and ^{18}F-derivatives of MTEP and MTEB (2-methyl-4-phenylethynyl-thiazole) has been described, allowing in vivo PET imaging in rhesus monkey.

The aim of our program was to identify a molecule with an improved tracer profile compared to the MPEP series, particularly a higher affinity, selectivity, and lower lipophilicity. Targeted chemical modifications of the original structure allowed the identification of ABP688, a derivative in which the aromatic ring of the MPEP series is replaced by a functionalized cyclohexenone moiety.

These modifications allowed a significant improvement of the physico-chemical properties such as a log *P* below 4 and a high water solubility (120 mg/L) compared to the previously published ligands bearing a substituted aromatic ring. As a result, ABP688 maintained an excellent selectivity and affinity for the allosteric site of the mGlu5 receptor while significantly improving physico-chemical properties. The radiosynthesis was straightforward, with the label introduced in the last step of the synthesis by alkylation of oxime **7** with methyl iodide yielding either [^{3}H]- or [^{11}C]ABP688[16] in high radiochemical yield and specific activity.

In vitro, ABP688 was found to be a highly potent functional inhibitor of the hmGlu5 receptor and to bind with high affinity to the human mGlu5 receptor (K_i = 3.5 nM). The characterization of the binding of the tritiated analog, [^{3}H]ABP688, showed a highly specific binding to the human (hmGluR5-expressing cells) or rat (whole brain) mGlu5 receptor. The binding was found to be fully displaceable by MPEP and M-MPEP, reversible, and with a very low level of non-specific binding. In membranes from whole rat brain, the saturation binding experiments with [^{3}H]ABP688 revealed a high B_{max} value of 0.87 ± 0.1 pmol/mg and a K_d of 1.9 nM. The profiling of ABP688 against a panel of CNS receptors further confirmed an excellent degree of selectivity for mGluR5.Autoradiography experiments in rat brain slices demonstrated that [^{3}H]ABP688 has a high specific binding to brain regions such as the striatum, cortex, and hippocampus with low or no binding to the cerebellum or to mid-brain regions, in line with the known distribution of the mGlu5 receptor.

In rats, despite an extensive plasma protein binding, [^{3}H]ABP688 rapidly and extensively penetrated the blood–brain barrier (BBB) with brain to plasma ratios of up to 20. The maximal brain concentrations were reached 5 min after iv injection. Importantly, despite extensive metabolism, no metabolites which could interfere with the imaging quality were detected in the brain.

In conclusion, the profile of ABP688 supports its selection for radiolabeling with [^{11}C] and further development as a PET tracer, to image mGlu5 receptors in vivo in the brain. The expected clinical benefits of such a tracer are multiple, from example receptor expression studies in patients, to receptor occupancy studies and clinical dose selection for drug candidates acting at mGlu5 receptors.

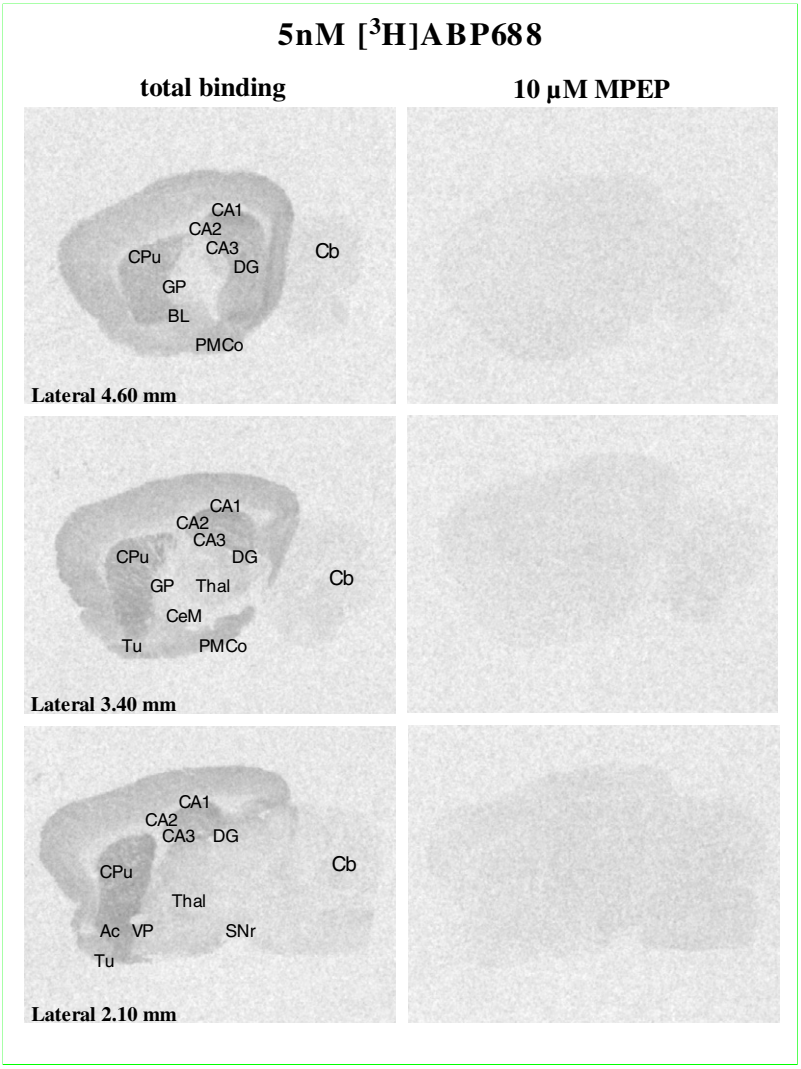

Figure 6. Representative autoradiographs obtained with [^{3}H]ABP688 in sagittal sections of rat brain slices taken at three different levels. Left panels, total binding of 5 nM [^{3}H]ABP688. Right panels, non-specific binding determined in the presence of 10 µM MPEP. Abbreviations: Ac, accumbens nucleus; BL, basolateral nucleus of the amygdala; CA1, CA2, CA3, fields CA1-3 of Ammon's horn; Cb, cerebellum; CeM, central nucleus of the amygdala; CPu, caudate putamen; DG, dentate gyrus; GP, globus pallidus; PMCo, postero medial cortical amygdaloid nucleus; SNr, substantia nigra reticulata; Thal, thalamic nuclei; Tu, olfactory tubercle; VP, ventral pallidum.

5. Experimental

5.1. General section

5.1.1. Chemicals. Reagents and solvents were purchased and used without further purification. Column chromatography was performed with Merck Silica Gel 60 (0.040–0.063 mm). Thin-layer chromatography to monitor reactions and to identify product-containing fractions was carried out using glass plates pre-coated with silica gel (60 F_{254}) and was developed in a UV-chamber (254 and/or 365 nm).

5.1.2. Analytics. High-resolution mass spectra were acquired on a 9.4T APEX III Fourier Transform mass spectrometer (Bruker Daltonik GmbH, Bremen, Germany) and mass spectra were obtained with a Micromass Platform II spectrometer in positive ESI mode. NMR spectra were measured at 300 K on a Varian 400 MHz (Varian Inc., Palo Alto, USA) or a DMX500 spectrometer (Bruker Biospin AG, Fällanden, Switzerland). All spectra were recorded in DMSO-d_6 using tetramethylsilane as internal standard.

5.2. Chemistry

5.2.1. Preparation of the labeling precursor 7 and ABP688 (2, Scheme 1)

5.2.1.1. 2-Methyl-4-(6-methyl-pyridin-2-yl)-but-3-yn-2-ol (3). To a solution of 2-bromo-6-methyl-pyridine (29.6 mL, 260 mmol) and 2-methyl-3-butin-2-ol (51 mL, 520 mmol, 2 equiv) in triethyl amine (720 mL) were added copper(I) iodide (4.0 g, 20.8 mmol, 0.08 equiv) and bis(triphenylphosphine)palladium(II)dichloride (7.3 g, 10.4 mmol, 0.04 equiv), and the resulting mixture was heated to 55 °C for 2 h. Then, the reaction mixture was cooled to room temperature (rt), poured onto ethyl acetate (3 L), and washed with brine (500

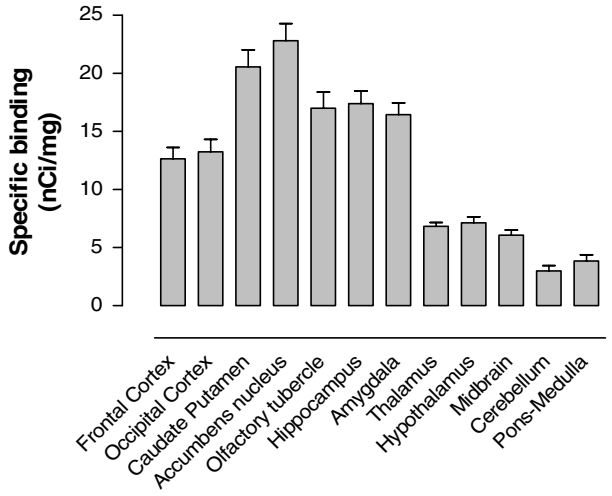

Figure 7. Quantitative analysis of the distribution of [^{3}H]ABP688-labeled sites in 12 regions of the rat brain. The data are expressed as nCi/mg tissue ± SEM, data are from three animals and each region was estimated at least nine times in total.

and 250 mL). The water phase was extracted with ethyl acetate (1 L), and the combined organic phases dried (Na_2SO_4), filtered, and concentrated in vacuo to yield the crude title compound. It was then filtered over a silica gel pad (1 kg, eluent hexanes/acetone 4:1 v/v) to yield 65.8 g of a brownish oil, which was used for the next step without further purification. ^{1}H NMR (400 MHz): 1.48 (s, 6H, 2× Me), 2.45 (s, 3H, Me), 5.57 (s, 1H, OH), 7.25 (app. t, J = 8.6 Hz, arom. H), 7.68 (t, J = 7.8 Hz, 1H, arom. H); MS $[M+H]^+$ 176.0.

5.2.1.2. 2-Ethynyl-6-methyl-pyridine (4). To a mixture of crude **3** (65.8 g, <260 mmol) in benzene (760 mL) was added freshly ground sodium hydroxide (8.9 g, 222 mmol, 0.85 equiv) and the mixture was heated to reflux for 1 h. Then, the mixture was cooled to rt, diluted with methyl *tert*-butyl ether (MTBE, 1.5 L), and filtered. The organic phases were washed with satd aq $NaHCO_3$ (2× 400 mL), the aqueous phases re-extracted with MTBE (0.5 L), the combined organic phases dried (Na_2SO_4), and the solvent carefully removed under reduced pressure (100 mbar, 40 °C bath temperature). The dark-brown residue was purified by column chromatography (1 kg SiO_2, eluent hexanes → hexanes/acetone 95:5 v/v), yielding 23.9 g (78% over two steps) of the title compound as a brownish liquid.[18]

5.2.1.3. 3-(6-Methyl-pyridin-2-ylethynyl)-cyclohex-2-enone (6). A mixture of **4** (17.0 g, 145 mmol), **5** (30.5 g, 174 mmol, 1.2 equiv), bis-(triphenylphosphine)-palladium(II)dichloride (4.08 g, 5.8 mmol, 0.04 equiv), and copper(I) iodide (2.21 g, 11.6 mmol, 0.08 equiv) in triethylamine (116 mL) and DMF (290 mL) was heated to 55 °C for 1 h. After completion of the reaction, the mixture was diluted with ethyl acetate (3 L) and washed with satd aq $NaHCO_3$ (500 and 250 mL). The water phase was extracted with ethyl acetate (1 L) and the combined organic phases were dried (Na_2SO_4), filtered, and concentrated in vacuo. The residue was purified by column chromatography (1.2 kg SiO_2, eluent hexane/ethyl acetate 3:1 v/v) and the fractions containing the title compound concentrated in vacuo to yield 23.1 g (75%) of the title compound as brownish crystals:

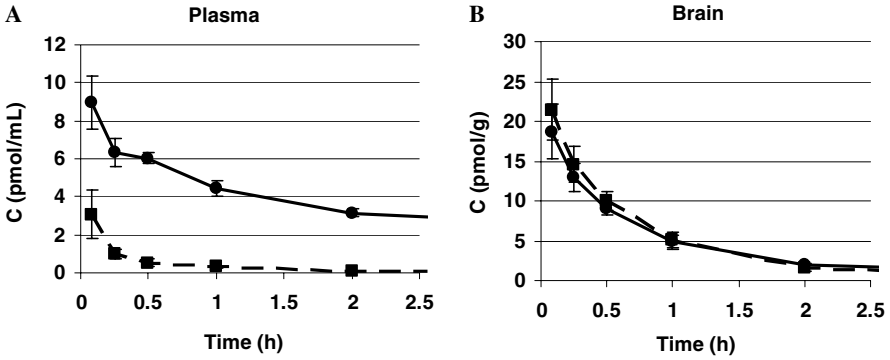

Figure 8. Plasma (A) and brain (B) concentrations of parent compound (squares) and total radioactivity (circles) after intravenous administration of 4 μg/kg [^{3}H]ABP688. Value are means ± SD, n = 3.

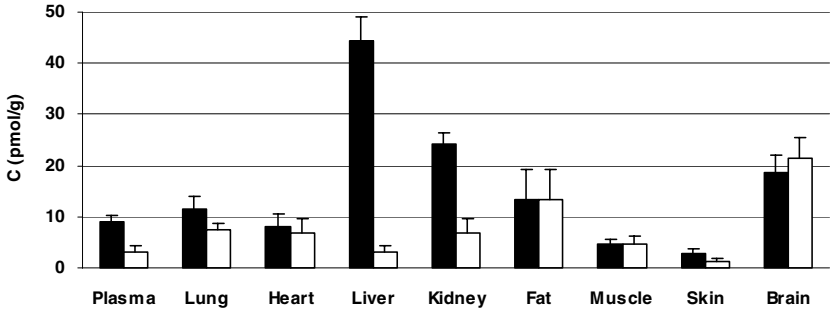

Figure 9. Tissue concentrations of radioactivity and parent drug. Mean concentrations (±SD, n = 3) of radioactivity (solid bars) and parent drug (open bars) 5 min. after intravenous administration of 4 μg/kg [3H]ABP688.

mp: 57–59 °C. ^{1}H NMR (400 MHz): 1.96–2.04 (m, 2H, CH_2), 2.41 (t, J = 6.6 Hz, 2H, CH_2), 2.50 (s, 3H, Me), 2.54–2.56 (m, 2H, CH_2), 6.27 (br d, J = 1.2 Hz, 1H, =CH–), 7.35 (d, J = 7.8 Hz, arom. H), 7.48 (3, J = 7.8 Hz, 1H, arom. H), 7.78 (t, J = 7.6 Hz, 1H, arom. H); MS $[M+H]^+$ 212.0.

5.2.1.4. 3-(6-Methyl-pyridin-2-ylethynyl)-cyclohex-2-enone oxime (7). A solution of **6** (200 mg, 0.95 mmol) and hydroxylamine hydrochloride (132 mg, 1.9 mmol, 2 equiv) in pyridine (9.5 mL) was stirred for 17 h at rt. After completion of the reaction, the solvent was removed in vacuo. The remaining pyridine was removed by dissolving the residue in toluene and re-evaporation (2× 100 mL). The resulting oil was dissolved in ethyl acetate (600 mL) and washed with satd aq $NaHCO_3$ (150 and 100 mL). The water phase was extracted with ethyl acetate (200 mL), and the combined organic phases dried (Na_2SO_4), filtered, and concentrated in vacuo. The residue was purified by column chromatography (250 g SiO_2, eluent toluene/acetone 6:1 v/v) and the fractions containing the desired compound concentrated to yield 196 mg (91%, 1.9:1 mixture of *E*/*Z*-isomers) of the title compound as light yellow crystals; mp 166–168 °C. ^{1}H NMR (500 MHz, *E*-isomer): 1.73–1.85 (m, 2H, CH_2), 2.40 (t, 2H, J = 5.7 Hz, CH_2), 2.57 (s, 3H, Me), 2.64 (t, J = 6.6 Hz, 2H, CH_2), 6.76 (br s, 1H, =CH–), 7.09 (d, 1H, J = 8.0 Hz, arom. H), 7.27 (m, 1H, arom. H), 7.55 (m, 1H, arom. H), 10.28 (s, 1H, NOH). ^{1}H NMR (500 MHz, *Z*-isomer): 1.89 (m, 2H, CH_2), 2.44 (t, 2H, J = 6.6 Hz, CH_2), 2.45 (t, 2H, J = 5.9 Hz, CH_2), 2.59 (s, 3H, Me), 7.11 (d, 1H, J = 8.1 Hz, arom. H), 7.29 (m, 1H, arom H), 7.38 (br s, 1H, =CH–), 7.56 (m, 1H, arom. H), 10.02 (s, 1H, NOH). ^{13}C NMR (125 MHz, *E*-isomer): 20.8 (t), 21.6 (t), 24.3 (q), 29.2 (t), 90.2 (s), 91.6 (s), 122.8 (d), 124.3 (d), 124.3 (d), 126.8 (s), 136.6 (d), 142.3 (s), 155.9 (s), 159.0 (s). ^{13}C NMR (125 MHz, *Z*-isomer): 22.3 (t), 24.3 (q), 27.6 (t), 30.5 (t), 90.1 (s), 92.4 (s), 123.0 (d), 123.2 (d), 124.6 (d), 130.1 (s), 136.6 (d), 142.1 (s), 152.1 (s), 159.1 (s); HR-MS $[M+H]^+$ 227.11789 (calcd 227.11789).

5.2.1.5. 3-(6-Methyl-pyridin-2-ylethynyl)-cyclohex-2-enone *O*-methyl-oxime (ABP688, 2). A solution of **6** (1.06 g, 5 mmol) and *O*-methyl-hydroxylamine hydrochloride (460 mg, 5.5 mmol, 1.1 equiv) in pyridine (50 mL) was stirred for 64 h at rt. After completion of the reaction, the solvent was evaporated in vacuo. The remaining pyridine was removed by dissolving the residue in toluene and re-evaporation (2× 20 mL). The residue was then taken up in ethyl acetate (150 mL) and washed with satd aq $NaHCO_3$ (2× 25 mL), the aqueous phases were re-extracted with ethyl acetate (50 mL), and the combined organic phases dried (Na_2SO_4) and concentrated in vacuo. Purification by flash chromatography (80 g SiO_2, eluent toluene/ethyl acetate 9:1 v/v) yielded 1.08 g (90%, 1.5:1 mixture of *E*/*Z*-isomers) of the title compound as a pale yellow oil which solidified upon standing. ^{1}H NMR (500 MHz, *E*-isomer): 1.79 (m, 2H, CH_2), 2.40 (t, 2H, J = 6.4 Hz, CH_2), 2.54 (t, J = 6.6 Hz, 2H, CH_2), 2.56 (s, 3H, Me), 3.92 (s, 3H, OMe), 6.56 (d, 1H, J = 1.5 Hz, =CH–), 7.09 (d, 1H, J = 7.7 Hz, arom. H), 7.27 (m, 1H, arom. H), 7.55 (m, 1H, arom. H). ^{1}H NMR (500 MHz, *Z*-isomer): 1.88 (m, 2H, CH_2), 2.40 (dt, 2H, J = 1.5 and 5.9 Hz, CH_2), 2.44 (m, 2H, CH_2), 2.56 (s, 3H, Me), 3.88 (s, 3H, OMe), 7.10 (d, 1H, J = 7.7 Hz, arom. H), 7.16 (t, J = 1.7 Hz, 1H, =CH–), 7.27 (m, 1H, arom. H), 7.54 (m, 2H, arom. H). ^{13}C NMR (125 MHz, *E*-isomer): 20.8 (t), 22.1 (t), 24.6 (q), 29.4 (t), 62.0 (q), 89.5 (s), 92.1 (s), 122.7 (d), 124.5 (d), 127.4 (s), 130.8 (d), 136.3 (d), 142.5 (s), 155.4 (s), 159.0 (s). ^{13}C NMR (125 MHz, *Z*-isomer): 22.3 (t), 24.6 (q), 27.5 (t), 30.4 (t), 61.6 (q), 89.3 (s), 93.0 (s), 122.9 (d), 123.1 (d), 124.6 (d), 130.8 (s), 136.3 (d), 142.2 (s), 151.8 (s), 159.1 (s); HR-MS $[M+H]^+$ 241.13344 (calcd 241.13354).

5.2.1.6. [^{3}H]ABP688 (Scheme 2). Tritiated ABP688 was synthesized by forming the potassium salt of **7** (0.45 mg, 2 μmol) in anhydrous DMF with KHMDS (2 μmol, 0.5 M solution in toluene), followed by reaction with [^{3}H]-methyl iodide (0.66 μmol, solution in toluene) at 120 °C for 150 min. The product was obtained after purification by semi-preparative HPLC (Nucleosil 100-3 C-18 HD, 125 × 3 mm, water/acetonitrile 1:1 to 5:95 over 15 min., 1 mL/min, 40 °C) as an *E*/*Z*-mixture (ca. 4:1, retention times = 14.3 and 15.8 min). Radiochemical purity of the *E*/*Z*-mixture was 99.4%, specific activity 2.83 TBq/mmol (11.78 MBq/μg).

5.3. Pharmacology

5.3.1. Cell lines. The generation and the pharmacological characterization of the CHO and L(tk-) cell lines expressing recombinant human mGluR1 (hmGluR1) or human mGluR5 (hmGluR5), respectively, was described previously.[23,30] Cell culture was performed essentially as described by Flor et al.[30] Briefly, cells were cultured in glutamate-free medium composed of DMEM lacking L-glutamate (without phenol red, Gibco, #11880-028) containing a reduced concentration of 2 mM L-glutamine (Gibco, # 25030-024), supplemented with 0.046 mg/mL proline (Sigma, # P0380), 10% dialyzed fetal calf serum (Gibco, # 26300-061), and 50 mg/mL geneticin (G-418 sulfate, Gibco, #11811-031). Expression of hmGlu5a receptors in L(tk-) cells was induced by 1 μM dexamethasone (Sigma, # D-2915).

5.3.2. Phosphoinositol accumulation assay. Measurements of phosphoinositide hydrolysis in L-hmGlu5a or CHO-hmGlu1b cells were carried out by determination of inositol monophosphate accumulation in the presence of lithium essentially as published previously.[28,29] Details are available in the Supplementary Information.

5.3.3. Membrane preparation. Membranes of hmGluR5-expressing cells were custom prepared by CMT (Cell and Molecular Technologies, Phillipsburg, NJ, USA), according to a previously established protocol.[9]

Rat brain membranes were obtained from ABS (Analytical Biological Services, Wilmington, DE, USA). All cell membranes used for the receptor binding panel were obtained commercially from Perkin-Elmer (Boston, MA,

USA) or Euroscreen (Gosselies, Belgium). Details are available in the Supplementary information.

5.3.4. [^{3}H]-M-MPEP competition assays. Radioligand displacement assays utilizing [^{3}H]-M-MPEP were carried out essentially as described previously.[22] Details are available in the Supplementary information.

5.3.5. [^{3}H]ABP688 binding assays. Reactions were performed in 96-well microtiter plates in a final assay volume of 200 µl per well. The assay mixtures contained membranes, suspended in assay buffer composed of Na–Hepes, (30 mM), NaCl (110 mM), $MgCl_2$ (1.2 mM), KCl (5 mM), $CaCl_2{\cdot}2\ H_2O$ (2.5 mM) at pH 8.0 [^{3}H]ABP688, and other reagents were added at the concentrations given below. Samples were incubated at 37 °C (duration given below) and then filtered through glass-fiber filters (Unifilter-96 GF/C plate) utilizing a 96-well plate filtration unit (Inotech). The filters were rinsed five times with cold assay buffer and dried before the addition of a scintillation fluid (Ultimate Gold XR, Packard; 100 µl per well). The assay plates were then shaken for 2–3 h and subsequently counted in a liquid scintillation counter (Wallac 1450 Microbeta or Packard Topcount NXT). Individual determinations were performed in triplicate.

5.3.5.1. Kinetic studies. To assess the time course of association, mixtures of [^{3}H]ABP688 (0.4 nM) and membranes (ca. 20 µg/well, hmGluR5 40 µg/well) were incubated at 37 °C from 1 to 90 min prior to filtration. The time course of dissociation was assessed in membranes previously equilibrated with [^{3}H]ABP688 (0.4 nM) for 60 min, after which 10 µM M-MPEP was added 1–90 min prior to filtration. A mono-exponential model was used to derive the observed association (k_{obs}) and dissociation (k_{-1}) rate constants. The association rate (k_1) was calculated according to $k_1 = (k_{obs} - k_{-1})/[L]$, where [L] was the added radioligand concentration.

5.3.5.2. Saturation binding and displacement assays. Saturation binding was assessed by adding various concentrations of [^{3}H]ABP688 (0.2–50 nM) to the membranes (rat 40 µg/well, hmGluR5 15 µg/well). Samples were left to equilibrate at 37 °C for 60 min prior to filtration. Non-specific binding of [^{3}H]ABP688 was defined as the radioactivity of samples incubated in the presence of an excess of M-MPEP (10 µM). Samples for displacement studies contained a fixed concentration of [^{3}H]ABP688 (1.5 nM) and other ligands at desired final concentrations. The data from the kinetic and equilibrium binding experiments were analyzed by the appropriate non-linear curve fitting procedures using GraphPad Prism 3.03 software package (GraphPad Software Inc., San Diego, CA). Inhibition constants were calculated according to the Cheng–Prussoff relation.

5.3.6. Brain slice autoradiography. Male Sprague–Dawley rats (RA238, Iffa Credo, France; 190–220 g) were individually housed in macrolon Type II cages. The animal room was temperature-controlled and equipped with artificial illumination (6:00–18:00 h, lights on). The animals had free access to water and food (Ecosan, Eberle Nafag AG, Gossau, Schweiz), ad libitum.

Animals were killed by decapitation, the brains were removed and immediately frozen on dry ice and kept at −80 °C. Sagittal brain slices (10 µm) for ex vivo receptor autoradiography were cut from frozen brains with a microtome-cryostat and thaw-mounted on silane-coated microscope slides. Receptor autoradiography was performed according to the following procedure: after 30 min of pre-incubation at room temperature in KRH buffer (Krebs–Ringer Hepes buffer) containing 20 mM Hepes (2-[4-(2-Hydroxyethyl)-1-piperazinyl] ethanesulfonic acid), pH 7.4, 118 mM NaCl, 4.8 mM KCl, 2.5 mM $CaCl_2$, 1.2 mM $MgSO_4$, and 10 mM NaOH, the sections were incubated for 15 min at room temperature in KRH buffer, supplemented with 0.05 mg/mL BSA (bovine serum albumin) and 5 nM [^{3}H]ABP688 (70 Ci/mmol). Non-specific binding was determined in a set of adjacent slides by incubation in the presence of 10 µM MPEP. The washing of labeled sections was carried out as follows: three 20-min washes in the ice-cold KRH buffer (without ligand), 20 s in ice-cold 10 times diluted KRH buffer, and a brief dipping in ice-cold distilled water to remove salts. Finally, the sections were dried under a stream of cold air. Autoradiograms were generated by apposing the labeled tissues to BioMax MR Films (Eastman Kodak Company, Rochester, New York 14650) at 4 °C for 6 weeks. Sections were finally counterstained with 0.5% Cresyl violet and nuclei localized according to Paxinos and Watson.[31] Data from binding were analyzed by optic densitometry of BioMax MR Films using the computerized image analysis system (MCID, Imaging Research, St. Catherines, Ontario, Canada). For a given labeled region, the optic density (OD) corresponding to the total binding and non-specific binding was measured.

5.4. DMPK studies

5.4.1. In vitro blood distribution and protein binding. Fresh heparinized human and rat blood was used for blood distribution studies and to obtain plasma.

5.4.1.1. Blood distribution. Rat and human blood was spiked with [^{3}H]ABP688 to 5–500,000 pg/mL; blood cells and plasma were separated by centrifugation (1500*g*, 10 min, 37 °C). Blood distribution was measured at 37 °C with total radioactivity being quantified in both plasma and blood; hematocrite values were determined using microhematocrite capillaries (13,000*g*, 5 min, $n = 3$). The fraction of compound in plasma (f_P) was calculated as $f_P\ (\%) = (C_p/C_b) \times (1\text{-}H) \times 100$, where C_b is the concentration in blood, C_p is the concentration in plasma, and H is the hematocrite value.

5.4.1.2. Plasma protein binding. Plasma was spiked with [^{3}H]ABP688 to 50–500,000 pg/mL and submitted to ultrafiltration at 37 °C with a Centrifree® device (Amicon Inc., Beverly, MA, USA, molecular cut-off of 30 kDa). The total radioactivity was determined in the ultrafiltrate by liquid scintillation (Cu, concentration of unbound compound) and in the sample introduced

into the reservoir before ultrafiltration (C_p, total plasma concentration of compound). The unbound (f_u) fraction in plasma was calculated as f_u (%) = $C_u/C_p \times 100$.

5.4.2. In vitro biotransformation and metabolites

5.4.2.1. Liver microsomes. Liver microsomal pools were obtained from Gentest (Woburn, MA, USA, male Sprague–Dawley rat H501 lot 11, mixed gender Caucasian human H161 lot 24). [^{3}H]ABP688 (0.92 μmol/L) was incubated for 40 min at 37 °C with liver microsomes (0.2 mg protein/mL) in 0.1 M sodium phosphate buffer, pH 7.4, containing 4 mM UDPGA (Sigma, St. Louis, MO, USA), 1 mM β-NADPH (Sigma), 5 mM MgCl2 (Merck), and 12 μg/mL. Individual samples were analyzed on-line by HPLC with radioactivity detection for depletion of unchanged compound as well as formation of metabolites; intrinsic clearance was calculated for each species from the kinetic data of parent compound.

5.4.3. Disposition of [^{3}H]ABP688 in rat. Male Wistar rats, 220–250 g (Charles River), were used. The injection solution consisted of 28 μg [^{3}H]ABP688 dissolved in 7.0 mL EtOH/glucose 5% (1:99 v/v). The dose was injected (1 mL/kg) into the surgically exposed femoral vein under slight isoflurane anesthesia.

The rats (n = 3 per sampling time) were sacrificed by isoflurane inhalation, heparinized blood was collected and centrifuged to obtain plasma; tissues (lung, heart, liver, kidney, fat, muscle, skin, and brain) were dissected.

The radioactivity of all samples was measured by liquid scintillation counting (Tri-Carb liquid scintillation spectrometer Model A2200, Packard). The concentration of unchanged [^{3}H]ABP688 in plasma and tissue homogenate was determined by LC-RID with 5 μg of non-labeled ABP688 as internal standard: [^{3}H]ABP688 was separated from metabolites and endogenous compounds on a LC-18 column (Supelcosil 5 μm, 4.6 × 150 mm, 40 °C, 10 mM NH_4OAc–acetonitrile (45:55 v/v), 1.0 mL/min, UV-detection, λ = 312 nm).The peak corresponding to [^{3}H]ABP688 was collected and radioactivity quantified. Finally, the concentration of [^{3}H]ABP688 was calculated from the ratio of radioactivity in the eluate fraction and the area of the UV peak of non-radiolabeled ABP688.

Acknowledgments

The authors thank H. P. Müller, W. Inderbitzin, R. Felber (Chemistry); D. Fehlmann, E. Shuepbach (autoradiography); P. Guntz (animal PK); R. Masero, R. Lehmann (Radiochemistry) C. Stierlin, N. Reymann (in vitro pharmacology), J. Hamon, Y. Gezahegen, T. Luethi, L. Sampson, S. Staub, and S. Vidal (cross-selectivity panel)for excellent technical support, E. Francotte for stability testing and HPLC analysis, Analytics Department (G. Bovermann, L. Oberer) for assignment of isomers, K. Kaupmann, J. Heid, S.Vognsen, and D. Monna for [^{3}H]ABP688 binding assays, G. Bruin and M. Weiss for providing in vitro metabolism and protein binding data, S. Ametamey, L. Kessler, M. Honer, M. Wyss, A. Buck, and P. A. Schubiger (Center for Radiopharmaceutical Science of ETH, PSI and University Hospital Zürich) for constructive discussions, G. Bilbe, K. McAllister for support of the project.

Supplementary data

Supplementary data associated with this article can be found, in the online version, at doi:10.1016/j.bmc.2006.10.038.

References and notes

1. Pin, J. P.; Duvoisin, R. *Neuropharmacology* **1995**, *34*, 1.
2. Spooren, W.; Ballard, T.; Gasparini, F.; Amalric, M.; Mutel, V.; Schreiber, R. *Behav. Pharmacol.* **2003**, *14*, 257.
3. Gasparini, F.; Lingenhohl, K.; Stoehr, N.; Flor, P. J.; Heinrich, M.; Vranesic, I.; Biollaz, M.; Allgeier, H.; Heckendorn, R.; Urwyler, S.; Varney, M. A.; Johnson, E. C.; Hess, S. D.; Rao, S. P.; Sacaan, A. I.; Santori, E. M.; Velicelebi, G.; Kuhn, R. *Neuropharmacology* **1999**, *38*, 1493.
4. Spooren, W. P. J. M.; Vassout, A.; Neijt, H. C.; Kuhn, R.; Gasparini, F.; Roux, S.; Porsolt, R. D.; Gentsch, C. *J. Pharmacol. Exp. Ther.* **2000**, *295*, 1267.
5. Tatarczynska, E.; Klodzinska, A.; Chojnacka-Wojcik, E.; Palucha, A.; Gasparini, F.; Kuhn, R.; Pilc, A. *Br. J. Pharmacol.* **2001**, *132*, 1423.
6. Spooren, W.; Gasparini, F. *Drug News Perspect.* **2004**, *17*, 251.
7. Passchier, J.; Gee, A.; Willemsen, A.; Vaalburg, W.; van Waarde, A. *Methods* **2002**, *27*, 278.
8. Talbot, P. S.; Laruelle, M. *Eur. Neuropsychopharmacol.* **2002**, *12*, 503.
9. Gasparini, F.; Andres, H.; Flor, P. J.; Heinrich, M.; Inderbitzin, W.; Lingenhoehl, K.; Mueller, H.; Munk, V. C.; Omilusik, K.; Sierlin, C.; Stoehr, N.; Vranesic, I.; Kuhn, R. *Bioorg. Med. Chem. Lett.* **2002**, *12*, 407.
10. Patel, S.; Krause, S. M.; Hamill, T.; Chaudhary, A.; Burns, H. D.; Gibson, R. A. *Life Sci.* **2003**, *73*, 371.
11. Hamill, T. G.; Seiders, T. J.; Krause, S.; Ryan, C.; Sanabria, S.; Gibson, R. E.; Patel, S.; Cosford, N.; Roppe, J.; Yang, J.; King, C.; Hargreaves, R. J.; Burns, H. D. *J. Labelled Compd. Radiopharm.* **2003**, *46*, S184.
12. Yu, M.; Tueckmantel, W.; Wang, X.; Zhu, A.; Kozikowski, A. P.; Brownell, A.-L. *Nucl. Med. Biol.* **2005**, *32*, 631.
13. Hamill, T. G.; Krause, S.; Ryan, C.; Bonnefous, C.; Govek, S.; Seiders, T. J.; Cosford, N. D. P.; Roppe, J.; Kamenecka, T.; Patel, S.; Gibson, R. E.; Sanabria, S.; Riffel, K.; Eng, W.; King, C.; Yang, X.; Green, M. D.; O'Malley, S. S.; Hargreaves, R.; Burns, H. D. *Synapse* **2005**, *56*, 205.
14. Ametamey, S. M.; Kessler, L.; Honer, M.; Auberson, Y.; Gasparini, F.; Schubiger, P. A. *J. Labelled Compd. Radiopharm.* **2003**, *46*, S188.
15. Kokic, M.; Honer, M.; Ametamey, S. M.; Gasparini, F.; Andres, H.; Bischoff, S.; Flor, P. J.; Heinrich, M.; Vranesic, I.; Spooren, W.; Kuhn, R.; Schubiger, P. A. *J. Labelled Compd. Radiopharm.* **2001**, *44*, S231.
16. Ametamey, S. M.; Kessler, L. J.; Honer, M.; Wyss, M. T.; Buck, A.; Hintermann, S.; Auberson, Y. P.; Gasparini, F.; Schubiger, P. A. *J. Nucl. Med.* **2006**, *47*, 698.
17. Sashida, H.; Kato, M.; Tsuchiya, T. *Chem. Pharm. Bull.* **1988**, *36*, 3826–3832.

18. Sakamoto, T.; Nagata, H.; Kondo, Y.; Sato, K.; Yamanaka, H. *Chem. Pharm. Bull.* **1984**, *32*, 4866.
19. Mewshaw, R. E. *Tetrahedron Lett.* **1989**, *30*, 3753.
20. Bax, A.; Davis, D. G. *J. Magn. Reson.* **1985**, *63*, 207.
21. Hwang, T. L.; Shaka, A. J. *J. Am. Chem. Soc.* **1992**, *114*, 3157.
22. Pagano, A.; Ruegg, D.; Litschig, S.; Stoehr, N.; Stierlin, C.; Heinrich, M.; Floersheim, P.; Prezeau, L.; Carroll, F.; Pin, J.-P.; Cambria, A.; Vranesic, I.; Flor, P. J.; Gasparini, F.; Kuhn, R. *J. Biol. Chem.* **2000**, *275*, 33750.
23. Daggett, L. P.; Sacaan, A. I.; Akong, M.; Rao, S. P.; Hess, S. D.; Liaw, C.; Urrutia, A.; Jachec, C.; Ellis, S. B.; Dreessen, J.; Knoepfel, T.; Landwehrmeyer, G. B.; Testa, C. M.; Young, A. B.; Varney, M.; Johnson, E. C.; Velicelebi, G. *Neuropharmacology* **1995**, *34*, 871.
24. Halme, M.; Sjoholm, B.; Savola, J.-M.; Scheinin, M. *Biochim. Biophys. Acta* **1995**, *1266*, 207.
25. Shigemoto, R.; Nomura, S.; Ohishi, H.; Sugihara, H.; Nakanishi, S.; Mizuno, N. *Neurosci. Lett.* **1993**, *163*, 53.
26. Romano, C.; van den Pol, A. N.; O'Malley, K. L. *J. Comp. Neurol.* **1996**, *367*, 403.
27. Romano, C.; Sesma, M. A.; McDonald, C. T.; O'Malley, K.; Van den Pol, A. N.; Olney, J. W. *J. Comp. Neurol.* **1995**, *355*, 455.
28. Lin, F. F.; Varney, M.; Sacaan, A. I.; Jachec, C.; Daggett, L. P.; Rao, S.; Flor, P.; Kuhn, R.; Kerner, J. A.; Standaert, D.; Young, A. B.; Velicelebi, G. *Neuropharmacology* **1997**, *36*, 917.
29. Litschig, S.; Gasparini, F.; Rueegg, D.; Stoehr, N.; Flor, P. J.; Vranesic, I.; Prézeau, L.; Pin, J. P.; Thomsen, C.; Kuhnm, R. *Mol. Pharmacol.* **1999**, *55*, 453.
30. Flor, P. J.; Lindauer, K.; Puttner, I.; Ruegg, D.; Lukic, S.; Knopfel, T.; Kuhn, R. *Eur. J. Neurosci.* **1995**, *7*, 622.
31. Paxinos, G.; Watson, C. *The Rat Brain in Stereotaxic Coordinates*, 2nd ed.; Academic Press: San Diego, 1986.